Features for a Modern Strain–Gage Balance Data Analysis Software Tool

N. Ulbrich† and T. Volden‡

Amentum Services, Inc., Moffett Field, California 94035–1000

Required, recommended, and optional features are discussed that benefit preparation and evaluation of the load prediction equations in a strain–gage balance data analysis tool. First, milestones in the evolution of load prediction methods are reviewed so that suggested features can be put into a historical context. Afterwards, independent and dependent variable choices for the balance data analysis are discussed. Then, it is illustrated how three different metrics may be used for the identification of the root cause of an unwanted divergence of the load iterations that may be observed during an iterative load prediction. Finally, a list of features is provided to guide software development efforts.

Nomenclature

$a_0,\ a_1,\ a_2$	= fitted coefficients of a regression model of the force of a load cell
AF	= axial force of a force balance
$b_1,\ b_2,\ \ldots,\ b_{27}$	= coefficients of the math model of an axial force bridge output
$c_0,\ c_1,\ c_2$	= fitted coefficients of a regression model of the electrical outputs of a load cell
F	= force acting on a load cell
F_{max}	= capacity of a load cell
NF	= normal force of a balance
NF'	= positive constant normal force
NF''	= negative constant normal force
$N1$	= forward normal force of a force balance
$N2$	= aft normal force of a force balance
PM	= pitching moment of a balance
Q	= *Percent Contribution*
rAF	= electrical output of the axial force bridge of a balance after weight tare removal
rF	= electrical output of a load cell
RM	= rolling moment of a force balance
$rN1$	= electrical output of the forward normal force bridge of a force balance
SF	= side force of a balance
$S1$	= forward side force of a force balance
$S2$	= aft side force of a force balance
YM	= yawing moment of a balance
ξ	= iteration step index

I. Introduction

Strain–gage balances have been used for more than 60 years for the measurement of the loads that act on a wind tunnel model. A primary balance, for example, can measure all six load components to high levels of accuracy. Unfortunately, due to design and space constraints, balance bridges have to be attached in close proximity to interconnected parts of the balance. Because of this, the bridges respond to load components they were not intended to measure. Therefore, load combinations must be applied at different levels during a calibration experiment so that more complex interactions between an applied load and the bridge outputs can correctly be described in the load prediction equations of the balance.

The load prediction equations of a primary balance for a wind tunnel test need to precisely characterize the multivariate nature of the relationship between the loads and the electrical outputs of the balance

† Aerodynamicist, Amentum Services, Inc.

‡ Systems Engineer, Amentum Services, Inc.

bridges. Many advances in mathematics, programming languages, and computer hardware have been made since the load prediction equations were first defined in the late 1950s. These advances led to improvements in both data analysis and load prediction methods that allow six–component balances to satisfy accuracy requirements of today's wind tunnel customers.

Many wind tunnel facilities use balance data analysis methods that do not necessarily reflect the latest advances in our understanding of the balance load prediction process. In addition, it is difficult to make updates to an existing analysis software package because a significant amount of development time and testing may be required to revise its algorithms. Consequently, an analyst may have to continue the use of a legacy software package even though its analysis results may not be as transparent or accurate as results that could be achieved with more modern approaches.

During the past two decades the authors developed and continuously refined a software tool for strain–gage balance data analysis at NASA Ames Research Center. The tool is called BALFIT. It takes advantage of many improvements that were made to the balance load prediction process. Therefore, the authors were able to identify a list of features that could be implemented in a modern balance data analysis tool.

First, the evolution of balance load prediction methods is reviewed so that suggested features can be put into a historical context. Then, independent and dependent variable choices for the balance data analysis are discussed. Afterwards, the application of three metrics to balance data is used to demonstrate benefits of metrics that are less frequently applied in the balance community. Finally, required, recommended, and optional features are presented that can guide the development of a balance data analysis tool.

II. Evolution of Load Prediction Methods

Important milestones in the evolution of balance load prediction methods are summarized in Fig. 1. The development of load prediction methods started in the 1950s when six–component balances became available for wind tunnel tests. Engineers had to develop mathematical relationships between the loads and electrical outputs of the balance bridges so that loads could be predicted from outputs during a wind tunnel test.

Cook's technical note of 1959 defines both the math model of the bridge outputs and the load iteration scheme that was initially used for the prediction of balance loads (see Ref. [1]). *Cook's* process is an early version of the *Iterative Method* that is still in use today (see Fig. 1). The primary difference between *Cook's* process and the *Iterative Method* is the fact that the *Iterative Method* uses *global regression*† for the determination of the math model coefficients of the bridge outputs. *Cook's* method, on the other hand, determines coefficients by performing a sequential graphical analysis of balance calibration data (Ref. [1], pp. 4–5). This approach was possible because *Cook's* calibration data consisted of subsets that were designed to support specific math model terms (basic ideas of *Cook's* approach are illustrated in the paper's appendix by using the math model of the axial force bridge output of a balance as an example). Finally, a load iteration scheme is constructed from the math models of the outputs so that loads can be predicted from outputs during a wind tunnel test (Ref. [1], pp. 5–7). *Global regression* was not considered for the processing of balance data in the late 1950s and 1960s because (i) the *matrix solution*‡ of the least squares problem was not yet widely known and (ii) computer resources were limited.

Researchers also started using the *Non–Iterative Method* for the balance load prediction in the 1960s. This alternate approach directly determines math models of the loads from the bridge outputs of balance calibration data. Therefore, no load iterations are required. However, linear or massive near–linear dependencies between math model terms were not rigorously investigated before the 2000s. This omission occasionally lead to incorrect load predictions when the regression model of a load was applied. The authors believe that this observation is one of the reasons why the *Iterative Method* became the preferred method for the balance load prediction in North American wind tunnels.

Significant advances were made in the 1970s that greatly benefited the analysis of balance calibration data (see Fig. 1). First, *Galway* of NRC Canada recognized the advantage of applying the *matrix solution*‡ of the least squares problem to balance calibration data (Ref. [7], p. 13, Eq. (36)). He also understood benefits

† The terminology *global regression* indicates that a single least squares fit is used to simultaneously determine all coefficients of the multivariate regression model of a dependent variable of balance calibration data.

‡ The *matrix solution* of the least squares problem is an application of the *Moore-Penrose* pseudo inverse that British physicist and Nobel Prize laureate *R. Penrose* first proposed in 1956 (Ref. [2]).

of the use of the *absolute value function*[†] in regression models of data from balances with bi–directional outputs and extended the idea to higher–order terms (Ref. [7], pp. 21–23; Ref. [8], p. 5). Furthermore, he recommended the use of the natural zero as the global datum for the electrical output of a balance bridge (Ref. [7], p. 27; *Galway* uses the synonym *buoyant component offset* in that context). Finally, *Galway* developed a tare load iteration process. His algorithm was first published in 1999 (Ref. [9]). *AIAA's Internal Balance Technology Working Group* adopted *Galway's* algorithm for use with the *Iterative Method* (Refs. [10] & [17]). *Galway's* four ideas were first implemented with the *Iterative Method* because (i) the *Iterative Method* was *Galway's* preferred load prediction approach and (ii) the reliability problem of the load prediction equations of the *Non–Iterative Method* had not yet been solved. Finally, the development of minicomputers (PDP, VAX) in the 1970s made computational resources more accessible. Consequently, *global regression* analysis could more easily be applied to balance calibration data.

No significant improvements of balance load prediction methods appear to have been made in the 1980s. However, the personal computer and FORTRAN & BASIC compilers became widely available. Now, analysts could implement the more complex analysis algorithms that emerged in the 1970s. It became obvious in the 1990s that the use of the *Iterative Method* had to be standardized so that a wind tunnel customer could use a given set of load prediction equations at multiple wind tunnel facilities. This conclusion was one of the reasons why *AIAA's Internal Balance Technology Working Group* (IBTWG) was established (see Ref. [11], p. 85, p. 88). A major accomplishment of this group was the development of a standard description of the *Iterative Method*. This description was published in 2003 in the first edition of *AIAA's* Recommended Practice document on calibration and use of internal strain–gage balances (Ref. [10]).

Again, advances were made during the 2000s after many data analysts adopted IBTWG's description of the *Iterative Method* and more powerful programming languages and software tools became available (C++, IDL, Matlab, EXCEL, Design–Expert, Python). For example, *Parker et al.* started to use the principles of *Design of Experiments (DOE)* during both preparation and execution of balance calibration experiments (Refs. [12], [13]). The primary goal of these efforts was the reduction of the total number of data points needed for a manual calibration of a balance. In addition, *Ulbrich* applied *Singular Value Decomposition (SVD)* to balance calibration data in 2005/2006 to analytically determine regression model terms that a given data set supports (Ref. [14]). He recognized that *SVD* needs to be applied to a transformed set of independent variables of the balance calibration data in order to be effective (Ref. [14], p. 3; Ref. [19], App. 17, p. 360). The supported regression model is assembled step–by–step, i.e., *SVD* is applied whenever a new term is considered for the regression model. The new term is either retained or rejected depending on the result of the *SVD* analysis (Ref. [19], App. 17, p. 362). Furthermore, it was discovered in 2007 that unsupported regression model terms associated with the use of the *Iterative Method* could be identified by using the *Variance Inflation Factor (VIF)* as a test metric (Ref. [15], p. 4). This discovery also meant that *VIFs* could be used to assess the reliability of regression models of the loads that the *Non–Iterative Method* uses. Then, load predictions resulting from the application of the *Non–Iterative Method* could be made as reliable as load predictions resulting from the application of the *Iterative Method*.

It was observed in 2010 that a convergence instability sometimes appeared when *Galway's* original tare load iteration algorithm was used in combination with the *Non–Iterative Method*. Therefore, an improved version of *Galway's* tare load iteration algorithm was developed that avoids the instability. This new tare load iteration algorithm was first published in 2011 (for details see Refs. [16], [18], [19]).

A second edition of *AIAA's* Recommended Practice document on calibration and use of internal strain–gage balances was published in 2020 (Ref. [17]). In addition, a new implementation of the *Non–Iterative Method* was completed at NASA Ames Research Center in the same year. This new implementation made it possible to systematically compare the load prediction accuracies of the *Non–Iterative Method* with the load prediction accuracies of the *Iterative Method*. Since 2020, comparisons have been made for many types of balances and calibration load schedule designs. They showed beyond any doubt that the accuracies of the load prediction equations of the *Non–Iterative* & *Iterative Methods* are the same for all practical purposes as long as five conditions are met: (i) the given balance calibration data is suited for the application of *global regression*, (ii) bridge outputs are formatted as differences relative to the natural zeros of the bridges, (iii) loads are tare corrected, i.e., described as differences relative to the datum of zero absolute load, (iv) the

[†] The idea of using the *absolute value function* for the description of bi–directional bridge output characteristics appears to have originated in Europe (Ref. [8], p. 5).

same function classes are used to define regression models of the dependent variables, and (v) the selected regression models are free of unwanted linear or near–linear dependencies. The application of the load prediction equations of the *Non–Iterative Method* is less complex than the application of the equations of the *Iterative Method*. No iterations are needed. Each load is computed by simply evaluating an explicit equation that uses the electrical outputs of the balance bridges as input. A NASA Contractor Report became available in 2022 that describes both analytical background and practical use of the *Iterative* and *Non–Iterative Method* in great detail (Ref. [18]). A second edition of this report was published at the beginning of 2024 (Ref. [19]).

III. Independent and Dependent Variables

Different justifications for the selection of the independent & dependent variable sets of balance data exist. They are directly linked to the historical development of balance load prediction methods. The *Iterative Method*, for example, uses bridge outputs as dependent variables and loads as independent variables during the regression analysis of balance data. This choice can be traced back to *Cook's* Technical Note of 1959 where he concludes ... *Each bridge indicator reading, as a consequence of interactions, is a function of all six load components.* ... (taken from Ref. [1], p. 3). Many longtime users of the *Iterative Method* also believe that it is "logical" to use bridge outputs as dependent variables because the bridge outputs are "measured" while the loads are "applied" during the calibration. This belief and *Cook's* conclusion come from the *traditional approach* that many metrology organizations use for the reporting of calibration data. The primary mission of a metrology organization is the calibration of sensors that measure a single physical quantity. In addition, a sensor's electrical outputs may have highly linear characteristics. Then, a metrology organization would provide the following information to the sensor's end user: (i) the sensor's raw calibration data, (ii) the first derivative of the sensor's electrical output, i.e., the sensitivity, and (iii) a regression model of the sensor's electrical output. It remains the end user's responsibility to figure out how the sensor's calibration information should be used so that the predicted physical quantity meets given accuracy requirements.

Wright illustrates the *traditional approach* of a metrology organization with calibration data of a load cell (Ref. [20], p. 150). His example can be used to show connections between *traditional approach*, *Iterative Method*, and *Non–Iterative Method*. Equation (1) below defines the second order regression model of the electrical output of the load cell that is used in *Wright's* example. Symbol rF describes the outputs

$$\textit{regression model of the electrical output} \quad \Longrightarrow \quad rF \; = \; c_0 + c_1 \cdot F + c_2 \cdot F^2 \qquad (1)$$

given in units of $[mV]$, symbol F describes the forces given in units of $[lbf]$, and $c_0,\ c_1,\ c_2$ are the regression coefficients. Equations $(2a)$ to $(2c)$ below list coefficient values that are given in the calibration report of the load cell (copied from Ref. [20], p. 150). Independent calculations confirmed that these coefficients were

$$\textit{intercept} \quad \Longrightarrow \quad c_0 \; = \; -1.1888\text{E}{-04}\ [mV] \qquad (2a)$$
$$\textit{sensitivity} \quad \Longrightarrow \quad c_1 \; = \; +3.8715\text{E}{-01}\ [mV/lbf] \qquad (2b)$$
$$\textit{coefficient of the higher order term} \quad \Longrightarrow \quad c_2 \; = \; +1.8648\text{E}{-06}\ [mV/lbf^2] \qquad (2c)$$

obtained by using the first eleven data points for the analysis. The report also says that the eleven data points were recorded while outputs were increasing. Therefore, the report's regression model is, to some degree, load direction dependent. It works best if the forces on the load cell are gradually increasing.

In theory, a load iteration equation can be constructed from Eq. (1) if the influence of the higher order term F^2 is small. This requirement can be verified if the term's *Percent Contribution* is computed using an equation that is given in the literature (see Ref. [19], App. 16). The load cell's capacity F_{max} is *50* $[lbf]$. Then, after applying Eq. (16.13) from Ref. [19], the *Percent Contribution* of term F^2 is obtained. We get:

$$Q(F^2) \; = \; \frac{c_2 \cdot \{F_{max}\}^2}{c_1 \cdot F_{max}} \times 100\ \% \; = \; \frac{1.8648\text{E}{-06} \cdot 50^2}{3.8715\text{E}{-01} \cdot 50} \times 100\ \% \; \approx \; 0.024\ \% \qquad (3)$$

The *Percent Contribution* is very small. It is well below the threshold of *0.1* % that identifies terms of no importance (see Ref. [19], p. 351, Table 16–3). Nevertheless, a load iteration equation can still be defined even though F^2 may not be needed for an accurate load prediction. Then, after solving Eq. (1) for force F and introducing the iteration step index ξ, the load iteration equation shown in Eq. $(4a)$ below is obtained.

$$\textit{load iteration equation} \quad \Longrightarrow \quad F_{\xi+1} \; = \; (1/c_1) \cdot [\, rF - c_0 \,] - (c_2/c_1) \cdot {F_\xi}^2 \qquad (4a)$$

The initial guess F_0 of the force is zero. Therefore, the first two estimates of the force can easily be computed:

$$F_1 \;=\; (1/c_1) \cdot [\, rF - c_0 \,] \tag{4b}$$

$$F_2 \;=\; (1/c_1) \cdot [\, rF - c_0 \,] \;-\; (c_2/c_1) \cdot {F_1}^2 \;=\; (1/c_1) \cdot [\, rF - c_0 \,] \;-\; (c_2/c_1^3) \cdot [\, rF - c_0 \,]^2 \tag{4c}$$

Equations (5*a*) & (5*b*) below list coefficients of the load iteration equation that were obtained from the right–hand sides of Eqs. (2*b*) & (2*c*). Numerical tests showed that a convergence tolerance of *0.0001* % of

$$\textit{inverse of the sensitivity} \implies 1\,/\,c_1 \;=\; +2.5830\,\mathrm{E}{+}00\;[lbf\,/\,mV] \tag{5a}$$

$$\textit{scaled coefficient of the higher order term} \implies c_2\,/\,c_1 \;=\; +4.8167\,\mathrm{E}{-}06\;[1\,/\,lbf] \tag{5b}$$

load capacity is met after two iteration steps. Equation (4*a*) above can be interpreted as a one–component balance version of the load iteration equation that *Cook* first introduced in 1959 (see Ref. [1], Eq. (4*a*)) and that *AIAA's Internal Balance Technology Working Group* published in 2003 (see Ref. [10], Eq. (3.3.4)).

An alternate justification for the definition of the independent and dependent variables of a balance data set emerged during the last decade. It supports the variable definition choices of both the *Iterative* and *Non–Iterative Method*. The justification is derived from the fundamental idea that a unique, i.e., reversible mapping between the loads and bridge outputs of a balance must always exist (see Ref. [21], pp. 3–5). Then, any "load state" of a balance can be described by using either the loads or the bridge outputs (see also discussions in Ref. [19], p. 2, pp. 10–12). Consequently, an analyst has the freedom to select either the loads or the bridge outputs as the dependent variables during the balance data analysis.

The load cell data of Ref. [20] was also processed with the *Non–Iterative Method* to show its connection to the *traditional approach* of a metrology organization. This alternate analysis was possible because the outputs are given as differences relative to an output datum that describes zero load. Equation (6) below

$$\textit{regression model of the force} \implies F \;=\; a_0 \;+\; a_1 \cdot rF \;+\; a_2 \cdot rF^{\,2} \tag{6}$$

shows the chosen regression model of the force that acts on the load cell. Equations (7*a*) to (7*c*) list coefficients that were computed after using the first eleven calibration points as input for the regression analysis. Both

$$\textit{intercept} \implies a_0 \;=\; +3.0772\,\mathrm{E}{-}04\;[lbf] \tag{7a}$$

$$\textit{inverse of the sensitivity} \implies a_1 \;=\; +2.5830\,\mathrm{E}{+}00\;[lbf\,/\,mV] \tag{7b}$$

$$\textit{coefficient of the higher order term} \implies a_2 \;=\; -3.2120\,\mathrm{E}{-}05\;[lbf\,/\,mV^{\,2}] \tag{7c}$$

the regression model of the force, i.e., Eq. (6) and the second estimate of the force from the load iteration process, i.e., Eq. (4*c*) are second order polynomials. Therefore, an analytical connection must exist between their coefficients. Intercept a_0 is given in Eq. (7*a*) as +3.0772 E−04 [*lbf*]. It is 0.00062 % of the load cell's capacity of 50 [*lbf*]. Similarly, intercept c_0 is given in Eq. (2*a*) as −1.1888 E−04 [*mV*]. It is −0.00059 % of the output of 20 [*mV*] at load cell capacity that *Wright* reports (see Ref. [20]). It is concluded that both intercepts are very small. They can be neglected. Then, after replacing a_0 and c_0 in Eqs. (6) and (4*c*) with zero and comparing the remaining coefficients of Eq. (6) with those of Eq. (4*c*), we get:

$$a_1 \;\approx\; 1/c_1 \;=\; +2.5830\,\mathrm{E}{+}00\;[lbf\,/\,mV] \tag{8a}$$

$$a_2 \;\approx\; -\,(c_2/c_1^3) \;=\; -3.2136\,\mathrm{E}{-}05\;[lbf\,/\,mV^{\,2}] \tag{8b}$$

Numerical values given on the right–hand sides of Eqs. (8*a*) and (8*b*) were computed with the values for c_1 and c_2 that are listed on the right–hand sides of Eqs. (2*b*) and (2*c*). They show excellent agreement with the independently obtained values that are listed for a_1 and a_2 on the right–hand sides of Eqs. (7*b*) and (7*c*). These observations indicate that the regression model of the force, i.e., Eq. (6) and the load iteration equation, i.e., Eq. (4*a*) will lead to load values of compatible magnitude and accuracy.

It needs to be mentioned that a good reason exists to separate the balance calibration laboratory of an aerospace testing center from its metrology organization. Balances are unique sensors that simultaneously measure up to six physical quantities. This characteristic is not a good fit for a metrology organization because its primary mission may be the calibration of sensors that measure a single physical quantity.

Different metrics were applied in the past to screen balance data for problems and make load predictions more reliable. Three examples of these metrics are discussed in the next section. They may be used in parallel to diagnose load iteration convergence problems whenever the *Iterative Method* is applied.

IV. Assessment of Load Iteration Divergence

Unsupported terms in the regression model of a bridge output are often responsible for the divergence of the load iterations that the *Iterative Method* uses (Ref. [10], p. 11, 3rd paragraph). Then, an analyst must use a considerable amount of subject–matter knowledge in combination with past experience to identify and remove the term (or terms) that may be responsible for the iteration divergence. This kind of troubleshooting can be very time–consuming. Its success highly depends on an analyst's skills. Alternatively, it is possible to investigate load iteration divergence by applying analytical methods and metrics. For example, iteration divergence may be studied by using the *Lipschitz Constant* (see Ref. [19], App. 11). In addition, it is known that *Variance Inflation Factors* (*VIFs*) can be used to identify terms that are responsible for the divergence (Ref. [15], p. 4, 4th para.). Finally, an examination of the *Percent Contributions* of the higher–order terms of the regression model may also be useful when trying to identify unsupported terms (this metric is defined in Ref. [19], App. 16). The connection between load iteration divergence, *Lipschitz Constant*, *VIFs*, and *Percent Contributions* can be demonstrated by using calibration data of NASA's MK3C balance as an example.

The MK3C balance was manufactured by the Task/Able Corporation. It is a six–component force balance that measures five forces and one moment (N1, N2, S1, S2, AF, RM). The balance has a diameter of *2.0* inches and a total length of *11.25* inches. Some of the bridge outputs of the balance are known to be bi–directional. Table 1 below shows the load capacity of each load component. The balance calibration was

Table 1: Load capacities of NASA's MK3C balance ($lbf \equiv$ pounds of force).

$N1,\ lbf$	$N2,\ lbf$	$S1,\ lbf$	$S2,\ lbf$	$AF,\ lbf$	$RM,\ in{-}lbf$
900	900	450	450	500	1000

performed in 2023 at the NASA Ames Balance Calibration Laboratory using the manual process. A total of *141* data points were recorded that were distributed across *16* load series. Figure 2 shows the load schedule of the complete manual calibration. Single–component loads were applied to all load components. In addition, combined loadings were applied using the forward and aft normal forces and the forward and aft side forces (see load series 3, 4, 8, and 11 in Fig. 2). Therefore, the original calibration data set supports the cross–product terms $N1 \times N2$ and $S1 \times S2$ in the regression models of the six bridge outputs.

A subset of the calibration data was created that omits load series 8 & 11 of the original calibration data set. Figure 3 shows the calibration load schedule of this subset. No combined loadings of the two side force components are part of the subset. Therefore, it cannot support the $S1 \times S2$ term.

In the next step, the data of the subset was processed with regression models that included the unsupported $S1 \times S2$ term. Figure 4a shows load iteration results for this situation. The load iterations diverge. Figure 4b shows the result of the iteration convergence test. The upper bound of the *Lipschitz Constant* equals *4.0143*. This value is well above the threshold of *1.0* that defines the dividing line between convergence and divergence. Iteration convergence is anticipated whenever the upper bound is less than *1.0*. Consequently, the magnitude of the *Lipschitz Constant* confirms that convergence problems can be expected with the chosen regression models of the outputs. Figure 4c shows the *VIFs* of the regression model of the forward normal force bridge output $rN1$ as an example. The *VIFs* of three terms, i.e., $|S1|$, $|S1|$, and $S1 \times S2$ are well above the threshold of *20* that is often used to assess near–linear dependencies in regression models of balance data. Therefore, massive near–linear dependencies exist in the regression model. Furthermore, it is known that both positive and negative loads were applied to the side forces (see Fig. 3). Therefore, it is concluded that the large *VIFs* must be caused by cross–product term $S1 \times S2$. Finally, Fig. 4d shows the *Percent Contributions* of the regression models of the six bridge outputs of the balance. The magnitudes of the *Percent Contributions* of the term $S1 \times S2$ for the six regression models of the outputs are unusually large (from *20.31* % to *157.76* %). In theory, the higher–order term $S1 \times S2$ should only make a small contribution in the part of the iteration equation that changes with each iteration step. Therefore, it is concluded that cross–product term $S1 \times S2$ is most likely responsible for the divergence of the load iterations.

Figure 5a shows load iteration results after processing the subset with regression models that omitted the unsupported $S1 \times S2$ term. In this case, the load iterations show rapid convergence. It is also observed that the upper bound of the *Lipschitz Constant* equals *0.0394* (see Fig. 5b). This value is well below the threshold of *1.0* indicating that rapid convergence can be expected. Figure 5c shows the *VIFs* of the alternate regression model of the forward normal force bridge output. Now, all *VIFs* are well below the threshold of

20 that is traditionally used to assess regression models of balance data. Therefore, no massive near–linear dependencies exist in the model. Finally, Fig. 5d shows the *Percent Contributions* of the alternate regression models of the six bridge outputs. The magnitudes of the percent contributions of all higher–order terms are below *2.0* %. Therefore, no iteration convergence problems are expected.

The authors have observed that load iterations are not guaranteed to diverge if an unsupported term is used in the regression models of the bridge outputs. In other words, the convergence behavior of the load iterations is an unreliable indicator of the presence of unsupported terms. The impact of an unsupported term on the iterations may simply be too small if regression models have a large number of terms. This situation often exists if machine calibration data of a balance is analyzed. Therefore, it is critical to check if the *Lipschitz Constant* is close to *1.0*, or, if the *VIFs* of the terms indicate a near–linear dependency, or, if the *Percent Contributions* of the higher–order terms of the regression models of the outputs have unusually large values. Any one of these observations could indicate the presence of an unsupported term.

VIFs have been used since the 1970s for the assessment of near–linear dependencies in response surface models of multivariate data sets (see Refs. [4] to [6]). It was concluded at the NASA Ames Balance Calibration Laboratory that *VIFs* could also be used to screen regression models of the tare corrected loads for linear or near–linear dependencies that are caused by the presence of unsupported regression model terms. Once screened for dependencies, the load prediction equations of the *Non–Iterative Method* can be made as reliable as the load prediction equations of the *Iterative Method* as long as unsupported terms in the regression models of the tare corrected loads are analytically identified and removed.

V. List of Software Features

The evolution of key elements of balance data analysis methods was reviewed. Then, the *Lipschitz Constant*, *VIFs*, and *Percent Contributions* were discussed as examples of metrics that may be used to screen regression models for hidden problems. It remains to identify features to include in a data analysis tool. Each feature needs to be defined, its importance needs to be rated, and an estimate of the development effort needs to be provided. Implementations of many complex algorithms already exist in modern programming languages (e.g., *IDL*, *Matlab*, *Python*) which helps to reduce the development effort.

Figure 6 summarizes milestones in the development of NASA's BALFIT software. The authors included many features in the tool that make the balance data analysis process more transparent, repeatable, and reliable. In addition, the software was intentionally designed to support all major approaches that use *global regression* for the generation of the load prediction equations of a balance. BALFIT is applied on a regular basis to balance calibration data. The authors decided to use BALFIT's development milestones as the starting point for the identification of features that they consider important. Figure 7 lists features that the authors selected. They are organized in three groups: required features, recommended features, and optional features. The features can be summarized as follows:

Required Features *(development effort ≡ low to high)*

• *Global Regression* ⟹ should be used in combination with the matrix solution of the least squares problem for the analysis of balance calibration data. Then, the physical behavior of the balance is described with multivariate regression models that are determined for each dependent variable by using a global least squares fit. The effort required for the implementation of *global regression* is low.

• *Percent Contribution* ⟹ should be implemented as a test metric so that the relative impact of the chosen regression model terms can be assessed (for details see Ref. [19], App. 16). The effort required for the implementation of the *Percent Contribution* is low.

• *Near–linear Dependency Test* ⟹ should be implemented so that *VIFs* can be used to screen regression models for unsupported terms (see Ref. [19], App. 18). The effort required for the implementation of the near–linear dependency test is low as long as the developer has a solid background in matrix algebra.

• *Tare Load Iteration Algorithm* ⟹ should be implemented so that all calibration loads are described relative to the common datum of zero absolute load (see Ref. [19], App. 12, App. 13). Referencing calibration loads to zero absolute load will result in more precise descriptions of the loads and more accurate load prediction equations. The implementation of the tare load iteration process can be complex even if an analyst has a good understanding of the algorithm itself. Therefore, the development effort is high.

Recommended Features *(development effort ≡ medium to high)*

- *Singular Value Decomposition* (*SVD*) ⟹ should be used to make an analytical detection of supported terms for the regression model possible (for details see Ref. [19], App. 17, App. 19). *SVD* works with both the regression models that the *Non–Iterative* and the *Iterative Method* use. The development effort required is *medium to high* assuming that the developer has a background in the programming of matrix methods.
- *Load Iteration Convergence Test* ⟹ should be implemented if the *Iterative Method* is chosen for the balance load prediction (for details see Ref. [19], App. 11). Typical convergence test results are shown in Figs. 4b and 5b. The development effort is *medium to high* assuming that the developer has a background in the programming of matrix methods.

Optional Features *(development effort ≡ high to very high)*

- *Regression Model Search Algorithm* ⟹ may be implemented (see, e.g., Ref. [19], App. 19); algorithm greatly reduces the total effort needed for the calibration data analysis.
- *Automatic Analysis Report Generation Capability* ⟹ may be developed; capability greatly reduces the total effort needed for the reporting of analysis results.
- *Graphical User Interface* ⟹ may be developed; interface makes interaction between analyst and software tool more convenient.

The implementation of the second and third optional feature should only be attempted if an organization has a long–term need for balance data analysis services. The implementation requires a team of developers who know balance data analysis problems very well and have excellent programming skills.

VI. Summary

Balance data analysis software may need to be replaced when (i) existing computer software or hardware is no longer supported or (ii) laboratory staff changes occur. These situations represent a unique opportunity for a laboratory to critically evaluate existing capabilities of its data analysis process. Improvements could be implemented that make the analysis process less dependent on an analyst's skills, more transparent to both analyst and wind tunnel customer, and more efficient to use. Features that may help a balance calibration laboratory make good software development decisions were discussed. First, the evolution of balance data analysis methods was reviewed so that origins of the most important features can be understood. Afterwards, independent and dependent variable choices for the regression analysis of balance data were discussed. Then, benefits of the application of the *Lipschitz Constant*, *Variance Inflation Factor*, and *Percent Contribution* were demonstrated by using data from the calibration of a force balance as an example. Finally, a list of required, recommended, and optional features for a modern balance data analysis tool was presented.

Acknowledgements

The authors want to thank James Bell of NASA for reviewing the paper. The preparation of the paper was supported by NASA Ames Research Center under contract 80ARC022DA011.

References

[1] Cook, T. A., *A Note on the Calibration of Strain Gauge Balances for Wind Tunnel Models,* Royal Aircraft Establishment, Technical Note No: AERO.2631, Ministry of Aviation, London, Dec. 1959.

[2] Penrose, R., "On Best Approximate Solutions of Linear Matrix Equations," *Mathematical Proceedings of the Cambridge Philosophical Society*, Vol. 52, Issue 1, January 1956, pp. 17–19.

[3] Guarino, J. F., "Calibration and Evaluation of Multicomponent Strain–Gage Balances," paper presented at the NASA Interlaboratory Force Measurements Group Meeting, Jet Propulsion Laboratory (JPL), Pasadena, California, April 1964.

[4] Marquardt, D. W., "Generalized Inverse, Ridge Regression, Biased Linear Estimation, and Nonlinear Estimation," *Technometrics,* Vol. 12, No. 3, August 1970, pp. 591–612.

[5] Belsley, D. A., Kuh, E., Welsch, R. E., *Regression Diagnostics: Identifying Influential Data and Sources of Collinearity*, John Wiley & Sons, New York, 1980, pp. 92–94.

[6] Montgomery, D. C., Peck, E. A., and Vining, G. G., *Introduction to Linear Regression Analysis,* 4th ed., John Wiley & Sons, Inc., New York, 2006, p. 334.

[7] Galway, R. D., *A Comparison of Methods for Calibration and Use of Multi–Component Strain Gauge Wind Tunnel Balances,* National Aeronautical Establishment, National Research Council Canada / Conseil National de Recherches Canada, NRC No. 18227, Aero. Rep. LR–600, Ottawa, March 1980.

[8] Clark, H., Sink, J.-E., MacMaster, M., " The Enduring Role of TASK Balances in Wind Tunnel Testing at the National Research Council Canada," AIAA 2023–3894, paper presented at the AIAA Aviation 2023 Forum, San Diego, California, June 2023, p. 5.

[9] Galway, R. D., "A Consideration of Tare Weight Effects in Calibration and Use of Wind Tunnel Strain–Gauge Balances," The Second International Symposium on Strain–Gauge Balances, Bedford, England, 4–7 May, 1999.

[10] AIAA/GTTC Internal Balance Technology Working Group, *Recommended Practice: Calibration and Use of Internal Strain–Gage Balances with Application to Wind Tunnel Testing,* AIAA R–091–2003, The American Institute of Aeronautics and Astronautics, Reston, Virginia, 2003.

[11] Cahill, D. M., " The AIAA/GTTC Internal Balance Technology Working Group," paper presented at the *First International Symposium on Strain Gauge Balances*, NASA Langley Research Center, Hampton, Virginia, October 22–25, 1996, NASA/CP–1999–209101/PT1 (part 1), p. 85, p. 88.

[12] Parker, P. A., Morton, M., Draper, N., and Line, W., "A Single–Vector Force Calibration Method Featuring the Modern Design of Experiments," AIAA 2001–0170, 38th Aerospace Sciences Meeting and Exhibit, Reno, Nevada, January 2001.

[13] Parker, P. A., Liu, T., "Uncertainty Analysis of the Single–Vector Force Balance Calibration System," AIAA 2002–2792, 22nd AIAA Aerodynamic Measurement Technology and Ground Testing Conference, St. Louis, Missouri, June 2002.

[14] Ulbrich, N., and Volden, T., "Application of a New Calibration Analysis Process to the MK–III–C Balance," AIAA 2006–0517, paper presented at the 44th AIAA Aerospace Sciences Meeting, Reno, Nevada, January 2006, p. 3.

[15] Ulbrich, N., and Volden, T., "Regression Analysis of Experimental Data using an Improved Math Model Search Algorithm," AIAA 2008–0833, paper presented at the 46th AIAA Aerospace Sciences Meeting, Reno, Nevada, January 2008, p. 4.

[16] Ulbrich, N., "A Universal Tare Load Prediction Algorithm for Strain–Gage Balance Calibration Data Analysis," AIAA 2011–6090, paper presented at the 47th AIAA/ASME/SAE/ASEE Joint Propulsion Conference, San Diego, California, July/August 2011.

[17] AIAA/GTTC Internal Balance Technology Working Group, *Recommended Practice: Calibration and Use of Internal Strain–Gage Balances with Application to Wind Tunnel Testing,* AIAA R–091A–2020, The American Institute of Aeronautics and Astronautics, Reston, Virginia, 2020, revised and enlarged second edition of Ref. [10].

[18] Ulbrich, N., *Evaluation, Analysis, and Application of Internal Strain–Gage Balance Data,* NASA/CR–20210026455, contractor report, Jacobs Technology Inc., Moffett Field, California, December 2021.

[19] Ulbrich, N., *Evaluation, Analysis, and Application of Internal Strain–Gage Balance Data,* NASA/CR–20230014293, contractor report, Jacobs Technology Inc., Moffett Field, California, September 2023, revised and enlarged second edition of Ref. [18].

[20] Wright, C. P., *Applied Measurement Engineering – How to Design Effective Mechanical Measurement Systems*, Prentice–Hall, Inc., Englewood Cliffs, New Jersey, 1995, p. 150, Fig. 5.9 .

[21] Ulbrich, N., "Assessment of the Uniqueness of Strain–Gage Balance Load Predictions," AIAA 2016–4157, paper presented at the 32nd AIAA Aerodynamic Measurement Technology and Ground Testing Conference, Washington, D.C., June 2016.

Appendix
Sequential Graphical Analysis of Balance Calibration Data

Elements of *Cook's* sequential graphical analysis approach for balance calibration data are reviewed because basic ideas of his calibration design are still applied today. The discussion of *Cook's* approach also illustrates why the introduction of *global regression* greatly simplified the calibration data analysis.

Cook's approach was often used in the 1960s and 1970s to develop the load prediction equations of a six–component strain–gage balance (Ref. [1]). *Cook's* process is an early version of the *Iterative Method* (Ref. [19], App. 10). It determines coefficients of the math models of the bridge outputs by performing a sequential graphical analysis of balance calibration data (Ref. [1], pp. 4–5). This approach was possible because *Cook's* balance calibration design consisted of twenty–one data subsets. Table 2 below shows the calibration data subsets that *Cook* used as input for his data analysis approach. Either one or two load components are

Table 2: Definition of data subsets needed for *Cook's* analysis approach.

SET NUMBER APPLIED LOAD ➡	SET 1 *AF*	SET 2 *SF*	SET 3 *NF*	SET 4 *RM*	SET 5 *PM*	SET 6 *YM*
SET NUMBER APPLIED LOADS ➡	SET 7 *AF, SF*	SET 8 *SF, NF*	SET 9 *NF, RM*	SET 10 *RM, PM*	SET 11 *PM, YM*	
SET NUMBER APPLIED LOADS ➡	SET 12 *AF, NF*	SET 13 *SF, RM*	SET 14 *NF, PM*	SET 15 *RM, YM*		
SET NUMBER APPLIED LOADS ➡	SET 16 *AF, RM*	SET 17 *SF, PM*	SET 18 *NF, YM*			
SET NUMBER APPLIED LOADS ➡	SET 19 *AF, PM*	SET 20 *SF, YM*				
SET NUMBER APPLIED LOADS ➡	SET 21 *AF, YM*					

simultaneously applied within a data subset. The twenty–one subsets were explicitly designed to support the twenty–seven–term math model that was used for the analysis of six–component balance data before absolute value terms were introduced in the 1970s. *Cook's* math model consists of six linear terms, six quadratic terms, and fifteen cross–product terms. He implicitly assumed that bridge outputs are formatted as differences relative to the outputs at the beginning of each load series (see also the discussion of bridge output format *Difference Type 2* in Ref. [19], App. 6). Therefore, no intercept is needed. *Cook's* bridge output format choice also means that the impact of the weight of the calibration equipment on the bridge outputs is neglected. Equation (9) below shows, for example, the twenty–seven–term math model of the axial force bridge output of a six–component balance that *Cook's* data subsets support.

$$\begin{aligned} rAF \; = \; & b_1 \cdot AF \; + \; b_2 \cdot SF \; + \; b_3 \cdot NF \; + \; \ldots \; + \; b_6 \cdot YM \\ & + \; b_7 \cdot AF^2 \; + \; b_8 \cdot SF^2 \; + \; b_9 \cdot NF^2 \; + \; \ldots \; + \; b_{12} \cdot YM^2 \\ & + \; b_{13} \cdot \{AF \cdot SF\} \; + \; b_{14} \cdot \{AF \cdot NF\} \; + \; \ldots \; + \; b_{27} \cdot \{PM \cdot YM\} \end{aligned} \tag{9}$$

The same terms are used to define math models of the outputs of the remaining five balance bridges. The coefficients $b_1, \; b_2, \; \ldots, \; b_{27}$ of the math model of the axial force bridge output are the unknowns. In theory, they could be obtained by performing a single least squares fit if *global regression* would be applied to the calibration data that *Cook's* twenty–one data subsets describe. However, computer resources were limited when *Cook* defined his approach in the late 1950s. Therefore, he developed a sequential graphical analysis approach that uses combinations of data subsets for the determination of the coefficients.

Cook's approach can be illustrated by reviewing the determination of the five coefficients b_1, b_3, b_7, b_9, and b_{14} of the axial force bridge output as an example. First, data of Set 1 is used to obtain the coefficients b_1 and b_7. The axial force is applied as a single–component load during Set 1. Therefore, data of Set 1 only supports a simplified version of Eq. (9) that is defined in Eq. (10) below.

$$\mathit{Set\ 1} \quad \Longrightarrow \quad rAF \; = \; b_1 \cdot AF \; + \; b_7 \cdot AF^2 \tag{10}$$

Now, the axial force bridge output is plotted versus the axial force as shown in Fig. 8. Coefficient b_1 describes the slope of the plotted line. It remains to determine the coefficient b_7 of the quadratic term from the data of Set 1. Therefore, both sides of Eq. (10) are divided by the axial force. Equation (11) below shows the resulting equation. It can be interpreted as a straight line. Coefficient b_1 is the intercept. Coefficient b_7 is

$$rAF / AF \quad = \quad b_1 \; + \; b_7 \; \cdot \; AF \tag{11}$$

the slope. It can be computed using a graphical approach after the left–hand side of Eq. (11), i.e., rAF/AF, is plotted versus the axial force (see Fig. 9).

It is also known that the normal force is applied as a single–component load in Set 3. Therefore, data of Set 3 supports a simplified version of Eq. (9) that is defined in Eq. (12) below. Coefficient b_3 can directly

$$\textit{Set 3} \quad \Longrightarrow \quad rAF \quad = \quad b_3 \; \cdot \; NF \; + \; b_9 \; \cdot \; NF^2 \tag{12}$$

be obtained using graphical analysis after plotting the axial force bridge output versus the normal force. In addition, similar to the determination of coefficient b_7, coefficient b_9 can be obtained after dividing both sides of Eq. (12) by the normal force. The result is shown in Eq. (13) below. It can be interpreted as

$$rAF / NF \quad = \quad b_3 \; + \; b_9 \; \cdot \; NF \tag{13}$$

a straight line where coefficient b_9 represents the slope. Again, the slope is obtained using graphical analysis after plotting rAF/NF versus the normal force.

The coefficient b_{14} of term $AF \cdot NF$ still needs to be determined. It can be obtained after applying *Cook's* approach to data of Set 12. It is known that data of Set 12 supports terms that are constructed from both AF and NF. Therefore, a five–term math model can be used for its analysis:

$$\textit{Set 12} \quad \Longrightarrow \quad rAF \; = \; b_1 \cdot AF \; + \; b_3 \cdot NF \; + \; b_7 \cdot AF^2 \; + \; b_9 \cdot NF^2 \; + \; b_{14} \cdot \{AF \cdot NF\} \tag{14}$$

Set 12 has data that was recorded by varying the axial force while keeping the normal force at a constant non–zero value. Outputs of the axial force bridge of Set 12 can be plotted versus the axial force for constant normal force. In addition, the partial derivative of the axial force bridge output with respect to the axial force can be obtained by treating the normal force as a constant. Then, the following value is obtained:

$$NF \; = \; \textit{const.} \qquad \Longrightarrow \qquad \partial \, rAF / \partial AF \; = \; b_1 \; + \; 2 \; \cdot b_7 \cdot AF \; + \; b_{14} \cdot NF \tag{15}$$

Consequently, the partial derivative at zero axial force is given by the following relationship:

$$NF \; = \; \textit{const.} \; \& \; AF \; = \; 0 \quad \Longrightarrow \quad \partial \, rAF / \partial AF \; = \; b_1 \; + \; b_{14} \cdot NF \tag{16}$$

Furthermore, it is assumed that data of Set 12 is recorded for the required minimum of two constant values NF' and NF'' of the normal force. The first normal force is positive ($NF' > 0$). The second normal force is negative ($NF'' < 0$). Now, the axial force bridge output observed for NF' and NF'' can separately be plotted versus the axial force so that the slope $\partial \, rAF / \partial \, AF$ for each of the two lines can be obtained (see red dots in Fig. 10). It is also known from the earlier analysis of Set 1 that the slope $\partial \, rAF / \partial \, AF$ equals coefficient b_1 if the normal force is zero (see blue dots in Fig. 10). Finally, the three slopes $\partial \, rAF / \partial \, AF$ can be plotted versus the related normal force values NF', NF'', 0. The slope of the resulting straight line is described in Eq. (17) below and shown in Fig. 11. It is the graphical estimate of

$$b_{14} \quad = \quad \frac{\partial \, (\, \partial \, rAF / \partial \, AF)}{\partial \, NF} \quad = \quad \frac{\partial^2 \; rAF}{\partial \, AF \; \partial \, NF} \quad \approx \quad \frac{\Delta \, (\, \partial \, rAF / \partial \, AF)}{\Delta \, NF} \tag{17}$$

coefficient b_{14} of term $AF \cdot NF$. The graphical determination of the remaining twenty–two coefficients of the math model of the axial force bridge output and of the coefficients of the math models of the other five bridge outputs follows *Cook's* process steps that are described in this appendix.

The example illustrates both complexity and bookkeeping challenges associated with *Cook's* approach. It also reminds the reader why *Galway's* introduction of *global regression* to balance calibration data analysis represents such an important milestone (see Ref. [7]). First, *global regression* greatly simplifies the analysis task because the given calibration data set is processed using a single least squares fit for each dependent variable. It also allows for the global assessment of multivariate regression models of balance data by using metrics like, e. g., the *p*–value, the *t*–statistic, the standard error, and the *Variance Inflation Factor.* Finally, *global regression* makes it possible to systematically include absolute value terms in regression models of the dependent variables of balances with bi–directional bridge outputs.

DATE	ITERATIVE METHOD	NON-ITERATIVE METHOD	MATHEMATICS	PROGRAMMING LANGUAGES	COMPUTER HARDWARE	COMMENTS
1950s	MATH MODEL OF BRIDGE OUTPUT COOK's METHOD (1959)	MATH MODEL OF LOAD	**MATRIX SOLUTION OF LEAST SQUARES PROBLEM (1956)**	FORTRAN	MAINFRAME COMPUTER	MULTIVARIATE MATH MODEL OF BRIDGE OUTPUT IS DEFINED (see, e.g., Ref. [1])
1960s	GRAPHICAL METHOD INSTEAD OF REGRESSION ANALYSIS IS USED FOR THE DETERMINATION OF MATH MODEL COEFFICIENTS	METHOD IS APPLIED TO DATA OF PRIMARY AND AUXILIARY BALANCES. HOWEVER, LINEAR DEPENDENCIES BETWEEN MATH MODEL TERMS ARE NOT SYSTEMATICALLY EXAMINED. THEREFORE, UNRELIABLE LOAD PREDICTIONS ARE SOMETIMES OBSERVED DURING APPLICATION.				CALIBRATION EXPERIMENT IS DESIGNED TO SUPPORT SPECIFIC TERMS SO THAT GRAPHICAL DETERMINATION OF MATH MODEL COEFFICIENTS IS POSSIBLE (see, e.g., Refs. [1], [3])
1970s	NATURAL ZERO = OUTPUT DATUM TARE LOAD ITERATION ABSOLUTE VALUE TERMS **GLOBAL REGRESSION**		**VIF APPEARS IN THE LITERATURE (EARLY 1970s)**		MINICOMPUTER (PDP, VAX)	ANAYSIS RESULTS OF BALANCE CALIBRATION DATA ARE SIGNIFICANTLY IMPROVED (see, e.g., Refs. [7], [8], [9])
1980s				FORTRAN BASIC	PERSONAL COMPUTER	NO SIGNIFICANT IMPROVEMENTS
1990s	AIAA's INTERNAL BALANCE TECHNOLOGY WORKING GROUP					DEVELOPMENT OF "STANDARD" FOR THE APPLICATION OF ITERATIVE METHOD
2000	DESIGN OF EXPERIMENTS (DOE)					CALIBRATION DESIGN IMPROVEMENTS (Ref. [12])
2003	AIAA RECOMMENDED PRACTICE (1st ed., R-091-2003, [10])			C++ IDL MATLAB EXCEL DESIGN EXPERT PYTHON		"STANDARD" FOR THE APPLICATION OF ITERATIVE METHOD IS PUBLISHED
2006	APPLICATION OF SIMPLIFIED SVD TO REGRESSION MODELS OF BALANCE DATA ([14])					SIMPLIFIED SVD MAKES IT POSSIBLE TO IDENTIFY SUPPORTED MATH MODEL TERMS
2007	**LOAD ITERATION DIVERGENCE IS RELATED TO PRESENCE OF LARGE VIFs IN MATH MODEL**	**VIFs CAN BE USED TO IDENTIFY AND REMOVE MODEL TERMS THAT CAUSE UNWANTED DEPENDENCIES**				"DISCOVERY" SOLVES RELIABILITY PROBLEM OF NON-ITERATIVE METHOD (see Ref. [15])
2011		DEVELOPMENT OF RELIABLE TARE LOAD ITERATION FOR NON-ITERATIVE METHOD				TARE LOAD ITERATION INSTABILITY IS REMOVED (see Ref. [16])
2020	AIAA RECOMMENDED PRACTICE (2nd ed., R-091A-2020, [17])	NASA's IMPLEMENTATION BECOMES SUITABLE FOR PRODUCTION TESTING				RIGOROUS SIDE-BY-SIDE IMPLEMENTATION OF THE ITERATIVE & NON-ITERATIVE METHOD AT NASA AMES WIND TUNNELS
2022	NASA CONTRACTOR REPORT (1st ed., NASA/CR-20210026455, [18])					FIRST SIDE-BY-SIDE DESCRIPTION OF ITERATIVE & NON-ITERATIVE METHOD
2024	NASA CONTRACTOR REPORT (2nd ed., NASA/CR-20230014293, [19])					

Fig. 1 The historical evolution of strain-gage balance load prediction methods.

SERIES	POINTS	N1	N2	S1	S2	AF	RM
1	9	+N1 +3.7% to +92.5%	< ±10%	< ±10%	< ±10%	< ±10%	< ±10%
2	10	−N1 −92.7% to −3.8%	< ±10%	< ±10%	< ±10%	< ±10%	< ±10%
3	10	−N1 −91.4% to −2.5%	−N2 −91.1% to −2.2%	< ±10%	< ±10%	< ±10%	< ±10%
4	10	+N1 +2.4% to +91.3%	+N2 +2.2% to +91.1%	< ±10%	< ±10%	< ±10%	< ±10%
5	10	< ±10%	+N2 +3.3% to +92.2%	< ±10%	< ±10%	< ±10%	< ±10%
6	10	< ±10%	−N2 −92.4% to −3.5%	< ±10%	< ±10%	< ±10%	< ±10%
7	6	< ±10%	< ±10%	+S1 +7.2% to +96.1%	< ±10%	< ±10%	< ±10%
8	6	< ±10%	< ±10%	+S1 +4.6% to +93.5%	+S2 +4.2% to +93.1%	< ±10%	< ±10%
9	6	< ±10%	< ±10%	< ±10%	+S2 +6.6% to +95.5%	< ±10%	< ±10%
10	6	< ±10%	< ±10%	−S1 −96.8% to −7.9%	< ±10%	< ±10%	< ±10%
11	6	< ±10%	< ±10%	−S1 −94.1% to −5.3%	−S2 −93.5% to −4.6%	< ±10%	< ±10%
12	6	< ±10%	< ±10%	< ±10%	−S2 −95.8% to −7.0%	< ±10%	< ±10%
13	12	< ±10%	< ±10%	< ±10%	< ±10%	< ±10%	+RM +0.0% to +76.0%
14	13	< ±10%	< ±10%	< ±10%	< ±10%	< ±10%	−RM −76.0% to +0.0%
15	10	< ±10%	< ±10%	< ±10%	< ±10%	+AF +7.7% to +87.7%	< ±10%
16	11	< ±10%	< ±10%	< ±10%	< ±10%	−AF −84.3% to −4.3%	< ±10%

Fig. 2 Calibration load schedule of the MK3C force balance <u>before</u> the omission of load series 8 and 11 (red color ≡ single–component loads ; blue color ≡ two–component loads).

SERIES	POINTS	N1	N2	S1	S2	AF	RM
1	9	+N1 +3.7% to +92.5%	< ±10%	< ±10%	< ±10%	< ±10%	< ±10%
2	10	−N1 −92.7% to −3.8%	< ±10%	< ±10%	< ±10%	< ±10%	< ±10%
3	10	−N1 −91.4% to −2.5%	−N2 −91.1% to −2.2%	< ±10%	< ±10%	< ±10%	< ±10%
4	10	+N1 +2.4% to +91.3%	+N2 +2.2% to +91.1%	< ±10%	< ±10%	< ±10%	< ±10%
5	10	< ±10%	+N2 +3.3% to +92.2%	< ±10%	< ±10%	< ±10%	< ±10%
6	10	< ±10%	−N2 −92.4% to −3.5%	< ±10%	< ±10%	< ±10%	< ±10%
7	6	< ±10%	< ±10%	+S1 +7.2% to +96.1%	< ±10%	< ±10%	< ±10%
9	6	< ±10%	< ±10%	< ±10%	+S2 +6.6% to +95.5%	< ±10%	< ±10%
10	6	< ±10%	< ±10%	−S1 −96.8% to −7.9%	< ±10%	< ±10%	< ±10%
12	6	< ±10%	< ±10%	< ±10%	−S2 −95.8% to −7.0%	< ±10%	< ±10%
13	12	< ±10%	< ±10%	< ±10%	< ±10%	< ±10%	+RM +0.0% to +76.0%
14	13	< ±10%	< ±10%	< ±10%	< ±10%	< ±10%	−RM −76.0% to +0.0%
15	10	< ±10%	< ±10%	< ±10%	< ±10%	+AF +7.7% to +87.7%	< ±10%
16	11	< ±10%	< ±10%	< ±10%	< ±10%	−AF −84.3% to −4.3%	< ±10%

Fig. 3 Calibration load schedule of the MK3C force balance <u>after</u> the omission of load series 8 and 11 (red color ≡ single–component loads ; blue color ≡ two–component loads).

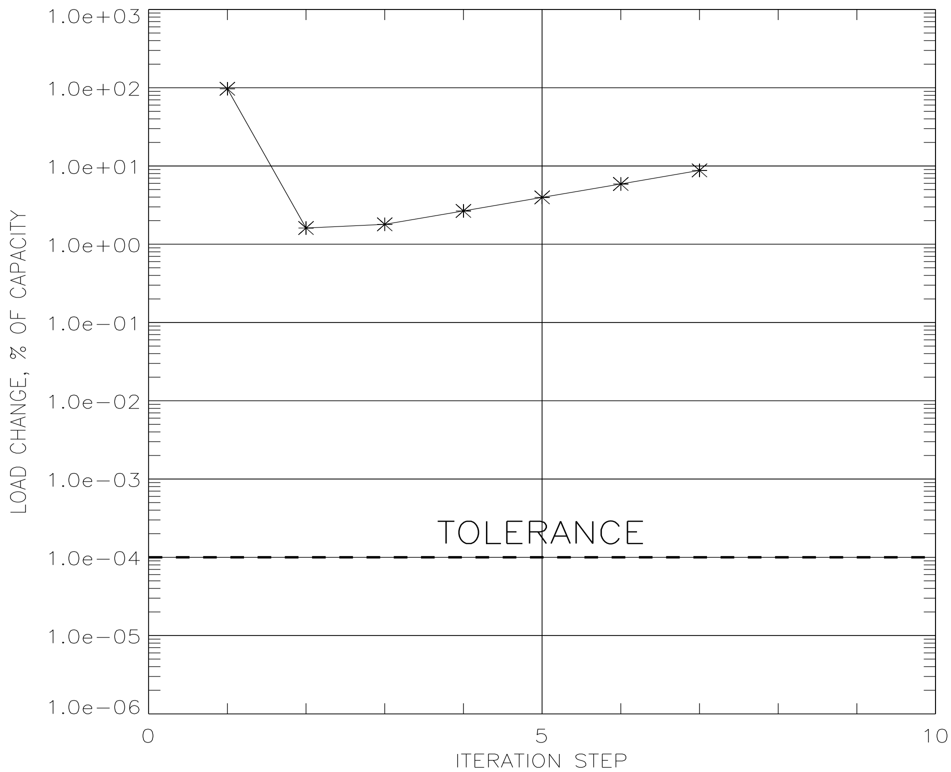

Fig. 4a Load iteration result <u>before</u> cross–product term $S1 \times S2$ is removed from the regression model of the calibration data set that omits load series 8 and 11 ($\Longrightarrow$ load iterations diverge).

CHOICE 1: LOAD VECTOR = 3/2 × LOAD CAPACITIES

N1 lbf	N2 lbf	S1 lbf	S2 lbf	AF lbf	RM in-lbf
+1350.00	+1350.00	+675.00	+675.00	+750.00	+1800.00

WARNING *** UPPER BOUND OF LIPSCHITZ CONSTANT = 4.0143 > 1.0 *** WARNING

Fig. 4b Upper bound of *Lipschitz Constant* <u>before</u> cross–product term $S1 \times S2$ is removed from the regression model of the calibration data set that omits load series 8 and 11.

PHYSICAL VARIABLES & UNITS – REGRESSION COEFFICIENT ESTIMATES AND STATISTICAL METRICS (rN1)

REGRESSION MODEL HIERARCHY CHARACTERISTICS = HIERARCHICAL

TERM INDEX	TERM NAME	COEFFICIENT VALUE	STANDARD ERROR	T–STATISTIC OF COEFFICIENT	P–VALUE OF COEFFICIENT	VARIANCE INFLATION FACTOR
1	INTERCEPT	−270.2059	+0.2462	−1097.7248	–	–
2	N1	+1.7941	+0.0005	+3980.7686	< 0.0001	+1.3532
3	N2	−0.0199	+0.0005	−43.8880	< 0.0001	+1.3547
4	S1	−0.0068	+0.0037	−1.8682	+0.0643	+6.8971
5	S2	−0.0059	+0.0070	−0.8340	+0.4060	+24.8376
6	AF	+0.0003	+0.0010	+0.2719	+0.7862	+1.0036
7	RM	+0.0004	+0.0004	+0.8890	+0.3759	+1.0001
8	|N1|	+0.0111	+0.0007	+16.8777	< 0.0001	+2.2112
9	|N2|	+0.0061	+0.0007	+9.3876	< 0.0001	+2.1794
10	|S1|	+0.0349	+0.0393	+0.8880	+0.3764	+740.4092
11	|S2|	+0.0513	+0.0550	+0.9332	+0.3527	+1427.4318
12	|AF|	+0.0011	+0.0012	+0.8855	+0.3778	+1.2281
13	|RM|	−0.0013	+0.0005	−2.5863	+0.0110	+1.1778
26	N1 x N2	+4.3500e−07	+1.5193e−06	+0.2863	+0.7752	+2.9814
35	S1 x S2	−0.0046	+0.0049	−0.9364	+0.3510	+2190.0970

Fig. 4c *Variance Inflation Factors* of the regression model terms of the forward normal force bridge output <u>before</u> cross–product term $S1 \times S2$ is removed from the model (red ≡ massive near–linear dependencies).

TERM	rN1	rN2	rS1	rS2	rAF	rRM
INTERCEPT	---	---	---	---	---	---
N1	[100.00 %]	−2.10 %	−0.12 %	+0.28 %	−0.13 %	−0.42 %
N2	−1.11 %	[100.00 %]	+0.19 %	−0.87 %	+1.34 %	−0.74 %
S1	−0.19 %	+3.5e−03 %	[100.00 %]	−0.64 %	+0.09 %	−0.07 %
S2	−0.16 %	−0.02 %	+0.14 %	[100.00 %]	−0.19 %	−0.04 %
AF	+8.7e−03 %	−9.9e−03 %	+0.03 %	+0.02 %	[100.00 %]	+0.33 %
RM	+0.03 %	−1.3e−03 %	+0.53 %	+0.20 %	−0.07 %	[100.00 %]
|N1|	+0.62 %	+0.07 %	−0.16 %	−0.02 %	−0.01 %	−0.35 %
|N2|	+0.34 %	+0.79 %	−0.14 %	+0.36 %	+0.05 %	+0.78 %
|S1|	+0.97 %	+0.34 %	−1.77 %	−0.55 %	+1.34 %	−1.17 %
|S2|	+1.43 %	+0.45 %	−3.94 %	+0.19 %	+1.79 %	−1.39 %
|AF|	+0.03 %	+0.02 %	+0.11 %	−0.16 %	+0.07 %	−0.03 %
|RM|	−0.09 %	−0.10 %	+0.41 %	+0.12 %	+0.04 %	−0.03 %
N1 x N2	+0.02 %	−0.14 %	−3.1e−03 %	+0.06 %	−0.15 %	+1.43 %
S1 x S2	−57.62 %	−20.31 %	+157.76 %	+30.21 %	−71.63 %	+45.80 %

Fig. 4d *Percent Contributions* of the regression model terms of the bridge outputs before cross–product term $S1 \times S2$ is removed (red ≡ very influential term; blue ≡ term of minor influence).

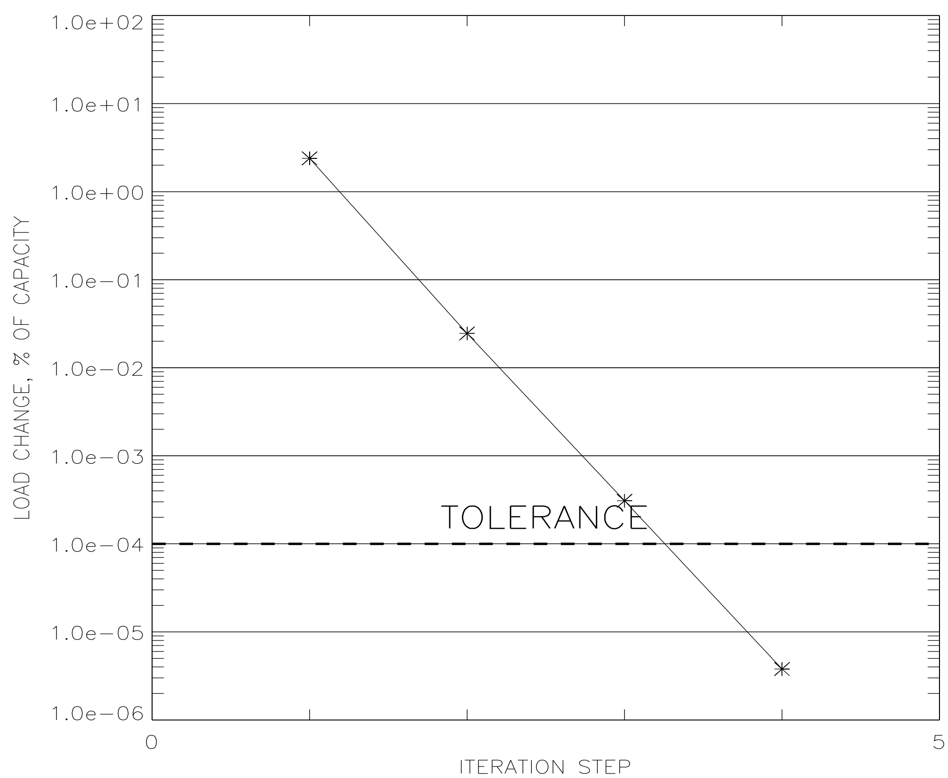

Fig. 5a Load iteration result after cross–product term $S1 \times S2$ is removed from the regression model of the calibration data set that omits load series 8 and 11 ($\Longrightarrow$ load iterations converge).

CHOICE 1: LOAD VECTOR = 3/2 × LOAD CAPACITIES

N1 lbf	N2 lbf	S1 lbf	S2 lbf	AF lbf	RM in-lbf
+1350.00	+1350.00	+675.00	+675.00	+750.00	+1800.00

UPPER BOUND OF LIPSCHITZ CONSTANT = 0.0394 < 1.0

LOWER BOUND OF NUMBER OF REQUIRED ITERATIONS FOR TOLERANCE OF 0.0001 % = 3

Fig. 5b Upper bound of *Lipschitz Constant* after cross–product term $S1 \times S2$ is removed from the regression model of the calibration data set that omits load series 8 and 11.

PHYSICAL VARIABLES & UNITS – REGRESSION COEFFICIENT ESTIMATES AND STATISTICAL METRICS (rN1)

REGRESSION MODEL HIERARCHY CHARACTERISTICS = HIERARCHICAL

TERM INDEX	TERM NAME	COEFFICIENT VALUE	STANDARD ERROR	T–STATISTIC OF COEFFICIENT	P–VALUE OF COEFFICIENT	VARIANCE INFLATION FACTOR
1	INTERCEPT	−270.0378	+0.1683	−1604.1597	–	–
2	N1	+1.7941	+0.0005	+3983.2975	< 0.0001	+1.3530
3	N2	−0.0199	+0.0005	−43.9794	< 0.0001	+1.3527
4	S1	−0.0037	+0.0014	−2.6289	+0.0097	+1.0043
5	S2	+0.0006	+0.0014	+0.4147	+0.6792	+1.0043
6	AF	+0.0003	+0.0010	+0.2753	+0.7836	+1.0036
7	RM	+0.0004	+0.0004	+0.8806	+0.3804	+1.0000
8	|N1|	+0.0109	+0.0006	+17.4789	< 0.0001	+1.9925
9	|N2|	+0.0060	+0.0006	+9.5127	< 0.0001	+2.0074
10	|S1|	−0.0019	+0.0015	−1.2426	+0.2165	+1.0942
11	|S2|	−0.0002	+0.0015	−0.1054	+0.9163	+1.0902
12	|AF|	+0.0009	+0.0012	+0.7190	+0.4736	+1.1826
13	|RM|	−0.0013	+0.0005	−2.8147	+0.0057	+1.1359
26	N1 x N2	+7.3205e−07	+1.4851e−06	+0.4929	+0.6230	+2.8514

Fig. 5c *Variance Inflation Factors* of the regression model terms of the forward normal force output after cross–product term $S1 \times S2$ is removed from the model (black ≡ no near–linear dependencies observed).

TERM	rN1	rN2	rS1	rS2	rAF	rRM
INTERCEPT	---	---	---	---	---	---
N1	[100.00 %]	−2.10 %	−0.12 %	+0.28 %	−0.13 %	−0.42 %
N2	−1.11 %	[100.00 %]	+0.20 %	−0.87 %	+1.34 %	−0.74 %
S1	−0.10 %	+0.03 %	[100.00 %]	−0.69 %	+0.20 %	−0.14 %
S2	+0.02 %	+0.05 %	−0.35 %	[100.00 %]	+0.03 %	−0.18 %
AF	+8.8e−03 %	−9.9e−03 %	+0.03 %	+0.02 %	[100.00 %]	+0.33 %
RM	+0.03 %	−1.4e−03 %	+0.53 %	+0.20 %	−0.07 %	[100.00 %]
|N1|	+0.61 %	+0.07 %	−0.13 %	−0.01 %	−0.02 %	−0.34 %
|N2|	+0.33 %	+0.78 %	−0.11 %	+0.36 %	+0.04 %	+0.79 %
|S1|	−0.05 %	−0.02 %	+1.03 %	−9.8e−03 %	+0.07 %	−0.36 %
|S2|	−4.5e−03 %	−0.05 %	−0.02 %	+0.94 %	+9.9e−03 %	−0.25 %
|AF|	+0.03 %	+0.01 %	+0.12 %	−0.15 %	+0.06 %	−0.03 %
|RM|	−0.10 %	−0.10 %	+0.42 %	+0.12 %	+0.03 %	−0.02 %
N1 x N2	+0.04 %	−0.13 %	−0.04 %	+0.05 %	−0.13 %	+1.42 %
S1 x S2	0	0	0	0	0	0

Fig. 5d *Percent Contributions* of the regression model terms of the bridge outputs after cross–product term $S1 \times S2$ is removed (red ≡ very influential term; blue ≡ term of minor influence).

Date	Milestones	Iterative Method (all load components)	Non-Iterative Method (single load component)	Non-Iterative Method (all load components)	References (see footnotes)
2005	- *SVD is applied to math models of balance data (start of development)* - *candidate math model search algorithm (start of development)* - *automatic report generation (start of development)*	2005			*AIAA-2005-4084*
2006	- *graphical user interface (start of development)*				*AIAA-2006-3434*
2007	- *VIFs are first used to screen regression model terms of outputs*				*AIAA-2008-0833*
2008	- *candidate math model search algorithm (major update)*				*AIAA-2008-0833*
2010	- *graphical user interface (major update)* - *non-iterative method (start of development, single load component is processed)* - *software design was made suitable for use at different laboratory sites*		2010		*AIAA-2010-0932* *AIAA-2010-4202*
2011	- *extended variable sets for iterative method (air balances)* - *universal tare load iteration algorithm*				*AIAA-2011-0949* *AIAA-2011-6090*
2012	- *bi-directional bridge output detection (start of development)*				*AIAA-2012-3320*
2013	- *simplified math model search algorithm*				*AIAA-2013-2996*
2016	- *control volume model of a strain-gage balance*				*AIAA-2016-4157*
2017	- *drag coefficient repeatability assessment (start of development)* - *weighted least squares approach (start of development)*				*AIAA-2017-0484* *AIAA-2017-4426*
2018	- *modeling of balance temperature effects* - *original Lipschitz convergence test (error in NASA TN D-6860 was not known)*				*Int. Bal. Symp.* *AIAA-2018-4109*
2019	- *drag coefficient repeatability assessment (major update)* - *experimental validation of temperature modeling* - *improved Lipschitz convergence test (error in NASA TN D-6860 was corrected)* - *precise definition of electrical output format choices* - *release of BALFIT Build 185 (latest version with graphical user interface)*				*AIAA-2019-1826* *AIAA-2019-2294* *AIAA-2019-3152* *AIAA-2019-3155*
2020	- *percent contribution for non-iterative method* - *non-iterative method (major update, all load components are processed)* - *common input file & report format (iterative & non-iterative method)* - *major refactoring of BALFIT's analysis module*		2020	2020	*AIAA-2020-0026* *Summer 2020*
2021	- *bi-directional bridge output detection (major update)*				*AIAA-2021-2968*
2022	- *weighted least squares approach (major update)* - *NASA/CR-20210026455 becomes publically available (Dec. 2022)*				*AIAA-2022-0138*
2023	- *balance interaction assessment (start of development)*	2023		2023	*AIAA-2023-1935*

Footnotes: References starting with *AIAA* refer to papers that were presented at conferences organized by the *American Institute of Aeronautics and Astronautics*. The reference *Int. Bal. Symp.* refers to a paper that was presented at the *11th International Symposium on Strain-Gauge Balances* in May 2018 in Cologne, Germany. The comment *Summer 2020* refers to major software updates were made in the summer of 2020.

Fig. 6 Milestones in the development of NASA's BALFIT software tool (from 2005 to 2023).

FEATURE	IMPORTANCE	EFFORT	COMMENTS
GLOBAL REGRESSION IN COMBINATION WITH THE MATRIX SOLUTION OF THE REGRESSION PROBLEM (Ref. [19], App. 9, App. 10)	REQUIRED	LOW	DEVELOPER NEEDS SOLID BACKGROUND IN MATRIX METHODS
PERCENT CONTRIBUTION (Ref. [19], App. 16)	REQUIRED	LOW	ALLOWS ANALYST TO ASSESS RELATIVE IMPACT OF REGRESSION MODEL TERMS
NEAR-LINEAR DEPENDENCY TEST (VIFs) (Ref. [19], App. 18)	REQUIRED	LOW	MAKES REGRESSION MODELS MORE RELIABLE WITHIN LOAD SCHEDULE CONSTRAINTS
TARE LOAD ITERATION ALGORITHM (Ref. [19], App. 12 or App. 13)	REQUIRED	HIGH	ALLOWS FOR MORE ACCURATE CALIBRATION LOAD DESCRIPTION
LINEAR DEPENDENCY TEST ("ROBUST" SVD) (Ref. [19], App. 17, App. 19)	RECOMMENDED	MEDIUM/HIGH	MAKES AUTOMATIC DETERMINATION OF SUPPORTED TERMS POSSIBLE
LOAD ITERATION CONVERGENCE TEST IF ITERATIVE METHOD IS APPLIED (Ref. [19], App. 11)	RECOMMENDED	MEDIUM/HIGH	ASSESSMENT OF GLOBAL LOAD ITERATION CHARACTERISTICS
REGRESSION MODEL SEARCH ALGORITHM (Ref. [19], App. 19)	OPTIONAL	HIGH	REDUCES TOTAL EFFORT NEEDED FOR BALANCE CALIBRATION DATA ANALYSIS
AUTOMATIC REPORT GENERATION (implemented in NASA's BALFIT software)	OPTIONAL	VERY HIGH (see footnote)	REDUCES TOTAL EFFORT NEEDED FOR REPORTING OF ANALYSIS RESULTS
GRAPHICAL USER INTERFACE (implemented in NASA's BALFIT software)	OPTIONAL	VERY HIGH (see footnote)	MAKES INTERACTION BETWEEN ANALYST AND SOFTWARE MORE CONVENIENT

Footnote: Development of "Automatic Report Generation" and "Graphical User Interface" makes sense for an organization that has a long-term need for balance data analysis services. It should be done by team of developers who (i) know balance data analysis problems very well and (ii) have excellent programming skills.

Fig. 7 List of required, recommended, and optional balance data analysis software features.

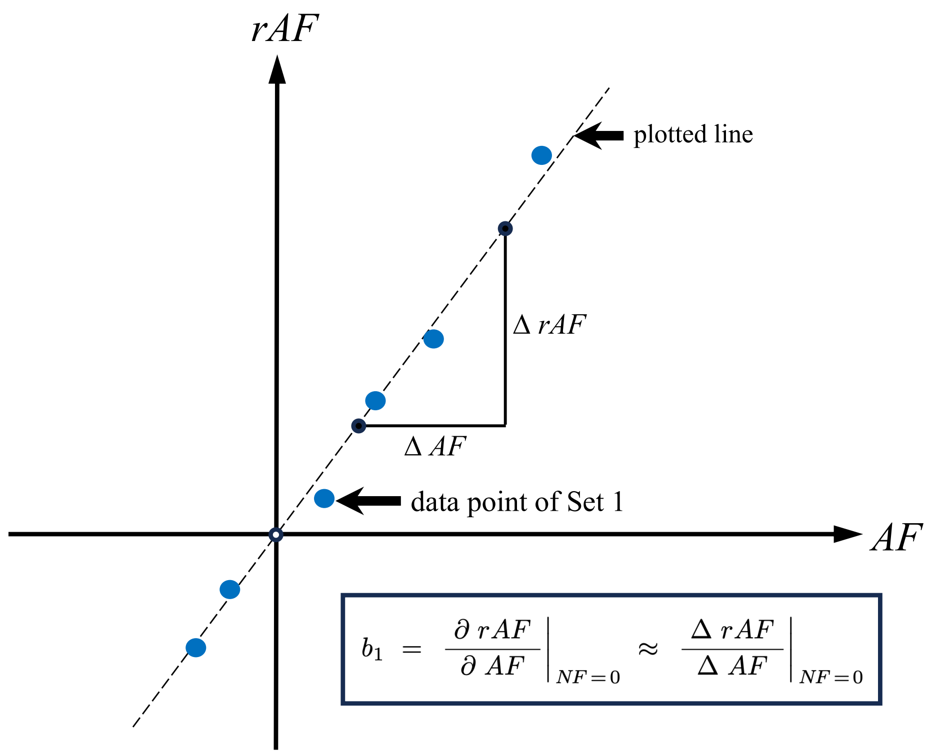

Fig. 8 Graphical determination of coefficient b_1 of term AF (blue dot = data point of Set 1).

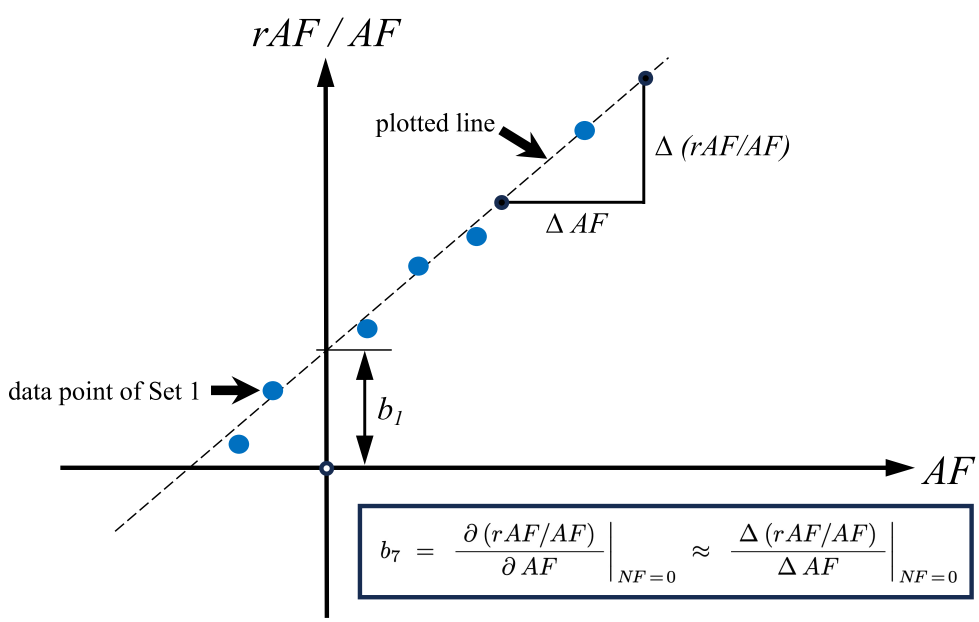

Fig. 9 Graphical determination of coefficient b_7 of term AF^2 (blue dot = data point of Set 1).

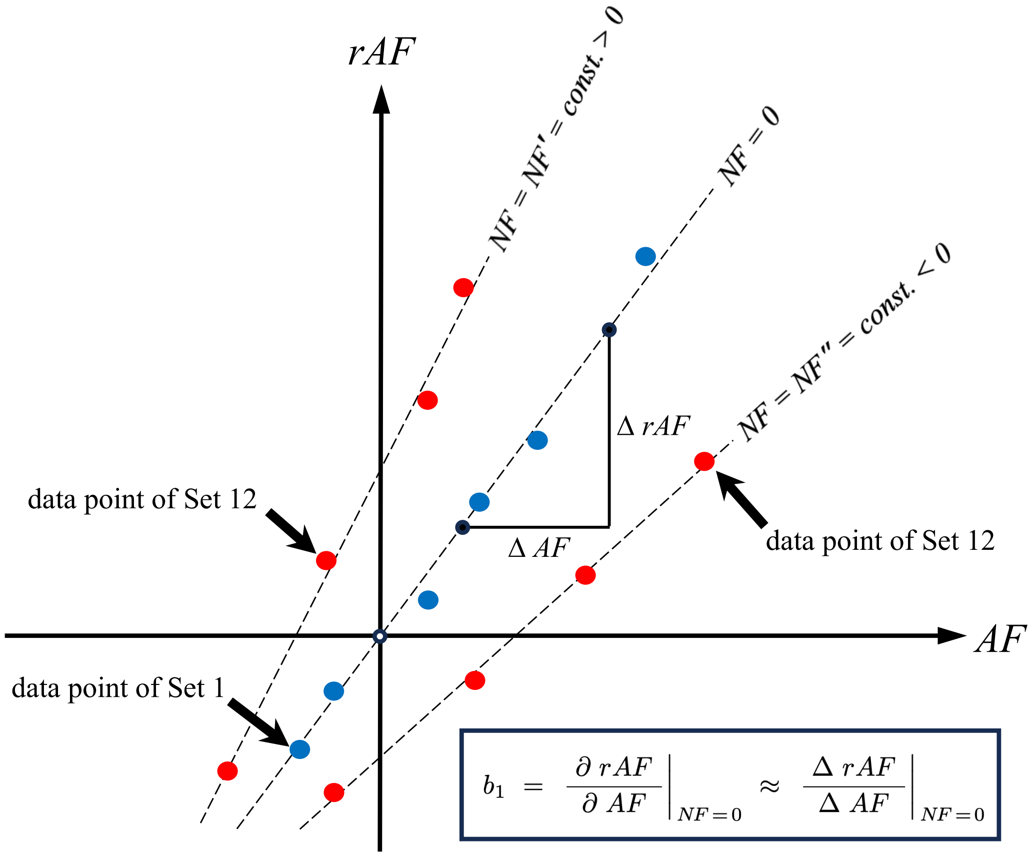

$$b_1 = \left.\frac{\partial\, rAF}{\partial\, AF}\right|_{NF=0} \approx \left.\frac{\Delta\, rAF}{\Delta\, AF}\right|_{NF=0}$$

Fig. 10 Graphical determination of the slope $\partial rAF/\partial AF$ for a constant normal force (red dot = data point of Set 12; blue dot = data point of Set 1).

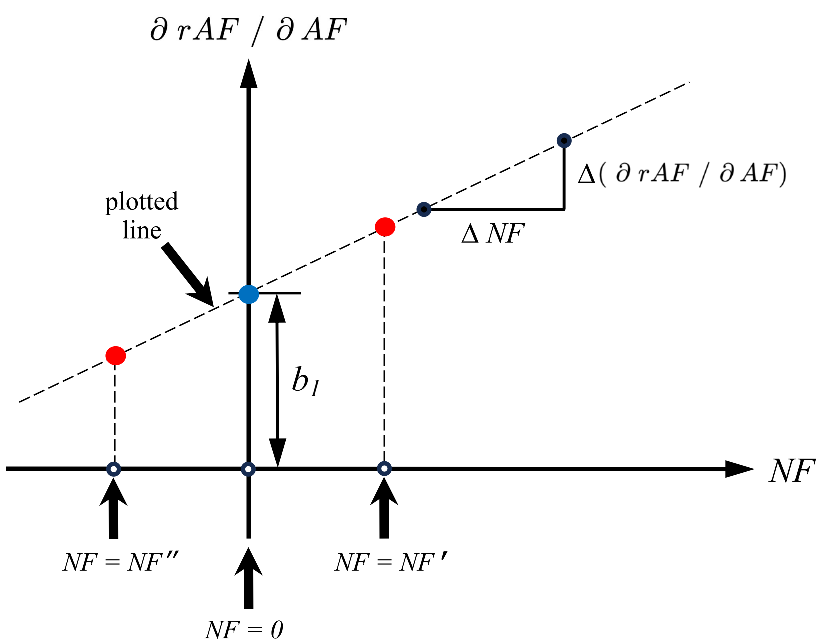

$$b_{14} = \frac{\partial\,(\partial\, rAF\,/\,\partial\, AF)}{\partial\, NF} = \frac{\partial^2\, rAF}{\partial\, AF\, \partial\, NF} \approx \frac{\Delta\,(\partial\, rAF\,/\,\partial\, AF)}{\Delta\, NF}$$

Fig. 11 Graphical determination of coefficient b_{14} of term $AF \cdot NF$.